CHAPTER IV

RESULTS AND DISCUSION:
$(1-x-y)Bi_{0.5}Na_{0.5}TiO_3–xBi_{0.5}K_{0.5}TiO_3–yBiFeO_3$

In this chapter, the results are presented on both powder and ceramic form of $(1-x-y)Bi_{0.5}Na_{0.5}TiO_3–xBi_{0.5}K_{0.5}TiO_3–yBiFeO_3$ (BNKFT), including microstructural, densification of materials and local structure analysis. Results of electrical properties, piezoelectric properties, ferroelectric hysteresis loop (P-E loop) and dielectric properties, of the materials are presented.

Introduction

Bismuth sodium titanate, $Bi_{0.5}Na_{0.5}TiO_3$ (abbreviated as BNT) has been considered to be a good candidate forlead-free piezoelectric ceramics because it has strong ferroelectricity at room temperature and a high Curie temperature T_c of 320 °C [58]. However, BNT ceramics have low piezoelectric properties, i.e. piezoelectric constant (d_{33}~58 pC/N) and an electromechanical coupling factor (k_p~0.15). Some studies have indicated that modifications to BNT ceramic can improve its piezoelectric properties. For instance, BNT-based compositions have been modified with $BaTiO_3$ (d_{33}=132 pC/N, k_p= 0.25) [88], $Bi_{0.5}K_{0.5}TiO_3$ (d_{33}=159 pC/N, k_p=0.30) [1], $NaNbO_3$ (d_{33}=88 pC/N, k_p=0.18) [6], $K_{0.5}Na_{0.5}NbO_3$ (d_{33}=90 pC/N) [89] etc. Among the solid solutions that have been developed so far the $(1-x-y)Bi_{0.5}Na_{0.5}TiO_3–xBi_{0.5}K_{0.5}TiO_3$ (BNKT) system has attracted considerable attention. However, the piezoelectric properties of these BNKT compositions are still far from satisfactory in terms of practical applications. Recently, it has been demonstrated that a ternary system design is favorable to improve piezoelectric and ferroelectric properties. Zhou et al. [9] reported that the $(1-x-y)Bi_{0.5}Na_{0.5}TiO_3–xBi_{0.5}K_{0.5}TiO_3–yBiFeO_3$ (BNKFT)ternary systems showed that superior electrical properties existed in the range of $0.18\leq x\leq 0.21$ and $0\leq y\leq 0.05$. The optimum values of d_{33} and k_p are 170 pC/N and 36.6% were observed from $0.79Bi_{0.5}Na_{0.5}TiO_3$-$0.18Bi_{0.5}K_{0.5}TiO_3$-$0.03BiFeO_3$ ceramics.

A literature survey revealed that the solid state reaction method has been used to prepare BNKFT ceramics. The pure phase was obtained by calcination and sintering temperatures above 900 °C and 1150 °C for 3-5 h. It is well known that this process of sample preparation is relatively simple, but it is time consuming, energy intensive and produces a poor quality ceramic. Recently, our previous work have successfully fabricated high quality different oxide ceramics such as $(Ba_{1-x}Sr_x)(Zr_xTi_{1-x})O_320]$, $Ba(Ti_{1-x}Zr_x)O_3$ [21], $(Pb_{1-x}Ba_xTiO_3)$ [22], $0.8Bi_{0.5}Na_{0.5}TiO_3$-$0.2Bi_{0.5}K_{0.5}TiO_3$[90] using the combustion technique. The advantages of this technique include inexpensive precursors, a simple preparation process, and resulting high-quality powders with a low firing temperature and a short dwell time [24, 25, 26]. Furthermore, from a survey of the literature, BNKFT powders and ceramics prepared by the combustion method have not been studied. Thus, in this work, $(1\text{-}x\text{-}y)Bi_{0.5}Na_{0.5}TiO_3$–$xBi_{0.5}K_{0.5}TiO_3$–$yBiFeO_3$ ($0.12\leq x\leq 0.24$ and $0\leq y\leq 0.07$) powders and ceramics were prepared by the combustion method. The effects of calcination and sintering temperatures and the change of the x and y content on the phase formation, microstructure and electrical properties of ceramics were also investigated.

Experimental

$(1\text{-}x\text{-}y)Bi_{0.5}Na_{0.5}TiO_3$-$xBi_{0.5}K_{0.5}TiO_3$-$yBiFeO_3$ ceramics ($0.12\leq x\leq 0.24$, fixed $x = 0.03$ and $0\leq y\leq 0.07$, fixed $y = 0.18$) (abbreviated as BNKFT-x/0.03 and BNKFT y/0.18) were prepared by the combustion technique. The starting materials used in this study were Bi_2O_3, Na_2CO_3, K_2CO_3, TiO_2 and Fe_2O_3. A stoichiometric amount of starting powders were weighed and ball-milled in ethanol for 24 h using a zirconia milling media. Drying was done at 120 °C for 6 h. The calcined powders were calcined between 600 and 800 °C for 2 h.The crystal structure of the calcined powders was detected by X-ray diffraction. The calcine powders were mixed with polyvinyl alcohol and pressed into discs with a diameter of 15 mm under 150 MPa. These pellets were subsequently sintered between 900 °C and 1075 °C for a 2 h dwell time with a heating/cooling rate of 5 °C/min.

Phase identification of calcined powders was investigated in 2θ ranges of 10 to 60° using an x-ray diffractometer (XRD). The lattice parameter was calculated

first by indexing the diffractogram according to hexagonal unit cell and the resulting parameters were then converted to the rhombohedral. The microstructure of all powders was observed using scanning electron microscopy (SEM) and transmission electron microscopy (TEM). The grain size of each sample was measured by a mean linear intercept method from the SEM micrographs. The theoretical density for each composition was calculated using the law of mixture and the densities of $Bi_{0.5}Na_{0.5}TiO_3$, $Bi_{0.5}K_{0.5}TiO_3$ and $BiFeO_3$ pure phases, which ware respectively, 5.99 g/cm^3 (JCPDS file no. 36-0340), 5.93 g/cm^3 (JCPDS file no. 36-0339) and 8.37 g/cm^3 (JCPDS file no. 20-0169). The relative density was obtained after measuring the external dimensions and weighing. This was then compared with the theoretical one. For electrical measurement, two parallel surfaces of sintered ceramics were polished and painted with silver paste for electrical contacts. The dielectric properties were measured at a temperature in the range of 25 °C - 450 °C with a measured frequency of 1 kHz using a 4263B LCR-meter connected to a high temperature furnace. Ferroelectric hysteresis loops were obtained using a ferroelectric test system (Radiant Technologies, Inc.). The piezoelectric coefficient (d_{33}) was poled under a DC field of 4 kV/mm at 120 °C in silicone oil for 30 min, using a quasistatic d_{33} meter (Berlincourt, Model CADT).

Result and Discussion

Effect of calcination temperature and content of x and y on crystal structure and microstructure of BNKFT powders

The XRD patterns of BNKFT-0.12/0.03 and BNKFT0.18/0.01 calcined powders at various temperatures are shown in Figure 30(a) and Figure 30(b), respectively. The X-ray analysis indicated that BNKFT-0.12/0.03 and BNKFT-0.01/0.18 calcined from 600 °C to 800 °C, had mainly a set peak with a major peak at (110). The crystal structure belonged to a rhombohedral phase, which could be matched with JCPDS file number 360340. The impurity phase of $K_4Ti_3O_8$was found in the BNKFT-0.12/0.03 and BNKFT-0.01/0.18 powders calcined below 750 °C. Above 750 °C the impurity phase disappeared and the sample showed a pure perovskite phase. The results of BNKFT-0.15/0.03, BNKFT-0.18/0.03, BNKFT-0.21/0.03, BNKFT-0.24/0.03, BNKFT-0/0.18, BNKFT-0.01/0.18, BNKFT-0.03/0.18, BNKFT-

0.05/0.18 and BNKFT-0.07/0.18 were similar to BNKFT-0.12/0.03 and BNKFT-0.18/0.01. The relative amounts of the perovskite phase were calculated by measuring major peak intensities of the perovskite phase. The percentage of perovskite is described by the following equation:

$$\%\, Perovskite\, phase = \left(\frac{I_{Perov}}{I_{Perov} + I_{K_4Ti_3O_8}} \right) \times 100 \qquad (10)$$

This well-known equation is widely employed in connection with the preparation of complex perovskite structurematerials [85]. I_{perov} and $I_{K_4Ti_3O_8}$ are the intensity of the (110) perovskite and the intensity of the highest $K_4Ti_3O_8$ peak. The percent of the perovskitephase of BNKFT-x/0.03and BNKFT-0.18/y powders at various calcination temperatures wascalculated and are listed in Table 6 and Table 7. The percentage of the perovskitephase in all samples increased with an increase of the calcination temperaturesand the highest percentage was observed in powders calcinedabove 750 °C. The lattice parameter a of BNKFT-x/0.03and BNKFT-0.18/y powders at different calcined temperatures (600-800 °C) were calculated from the (101), (012), (110), (003), (021), (202), (113), (211), (104) and (122) reflective peaks of XRD patterns and are listed in Table 6 and Table 7.

The lattice parameter a of all the samples increased with an increase of calcinations temperature. It was observed that at low calcining temperatures, the powders exist in a more strained form within the atomic entities in non-equilibrium positions, which relax to the equilibrium positions at higher temperature.

Figure 33(a–f) shows SEM photomicrographs of BNKFT-0.12/0.03 and BNKFT- 0.18/0.01 powders at different temperatures. In general, the particles are agglomerated and have a spherical morphologic shape. With an increase of calcination temperatures from 600°C to 800°C, the average primary particle size increase from 264 nm to 411 nm (for BNKFT-0.12/0.03) and 228 nm to 328 nm (for BNKFT-0.18/0.01), and the agglomeration measured from 493 nm to 691nm (for BNKFT-0.12/0.03) and 467 nm to 673 nm (for BNKFT-0.18/0.01), as seen in Figure 33(a–f)

and listed in Table 6 and Table 7. It is also of interest to point out that average particle size tended to increase with increased calcination temperatures. This is because of the occurrence of hard agglomeration with a strong inter-particle bond within each aggregate which is the result of the firing process [91]. The SEM results of BNKFT-0.15/0.03, BNKFT-0.18/0.03, BNKFT-0.21/0.03, BNKFT-0.24/0.03, BNKFT-0/0.18, BNKFT-0.03/0.18, BNKFT-0.05/0.18 and BNKFT-0.07/0.18were similar to BNTFT-0.12/0.03 and BNKFT-0.18/0.01, as listed in Table 6 and Table 7.

The optimum calcination temperature of all samples was found at 750°C for 2 h, and it was then that the amounts of x and y on the crystal structure and microstructure were examined. The XRD diffraction patterns of BNKFT-x/0.03 and BNKFT-0.18/y powders in the range of 10°–60°are shown in Figure 32(a) and 32(b), respectively. It has been verified that all the samples are of a single-phase perovskite structure. All the peaks of the solid solution system were indexed to the rhombohedral structure and the pattern matching based on JCPDS file no. 36-0340. The position corresponding to the characteristic (110) peak shifts towards a lower angle as the x and y content are increased in the solid solution, as shown in Figure 32(a) and 32(b). The lattice parameter of aincreased with increasing x and y content, as listed in Table 6 and Table 7. It is because the higher radius (1.64 Å) of the K^{+}ion replaces Na^{+} (1.39 Å) and (0.65 Å) of the Fe^{3+}replaces Ti^{4+}(0.61 Å) resulting in the increase of the effective ionic radius of the A- and B-site respectively. The distortion of the unit cell induces strain in the lattice that may induce an increase of lattice parameter a [19].

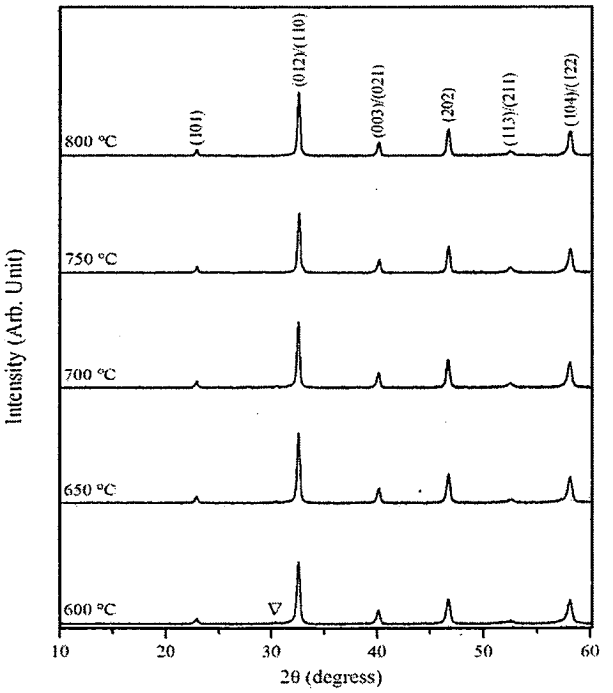

(a)

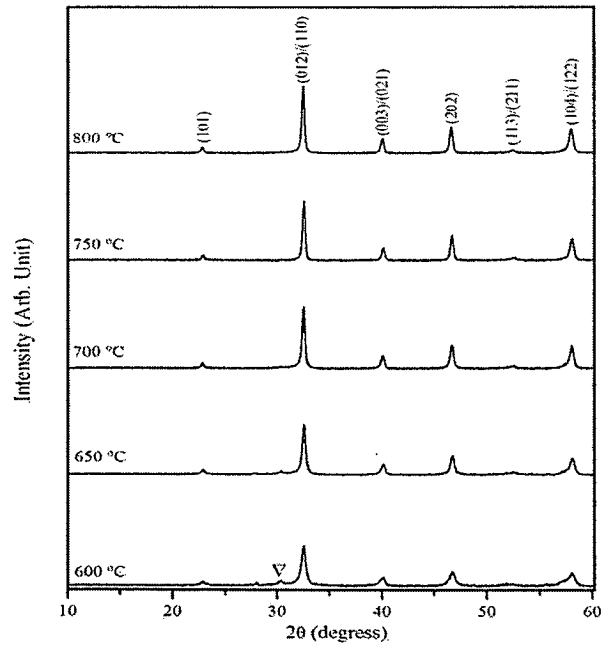

(b)

Figure 30 XRD patterns of (a) BNKFT-0.12/0.03 and (b) BNKFT-0.18/0.01 powders calcined at various temperatures for 2 h: (∇ $K_4Ti_3O_8$)

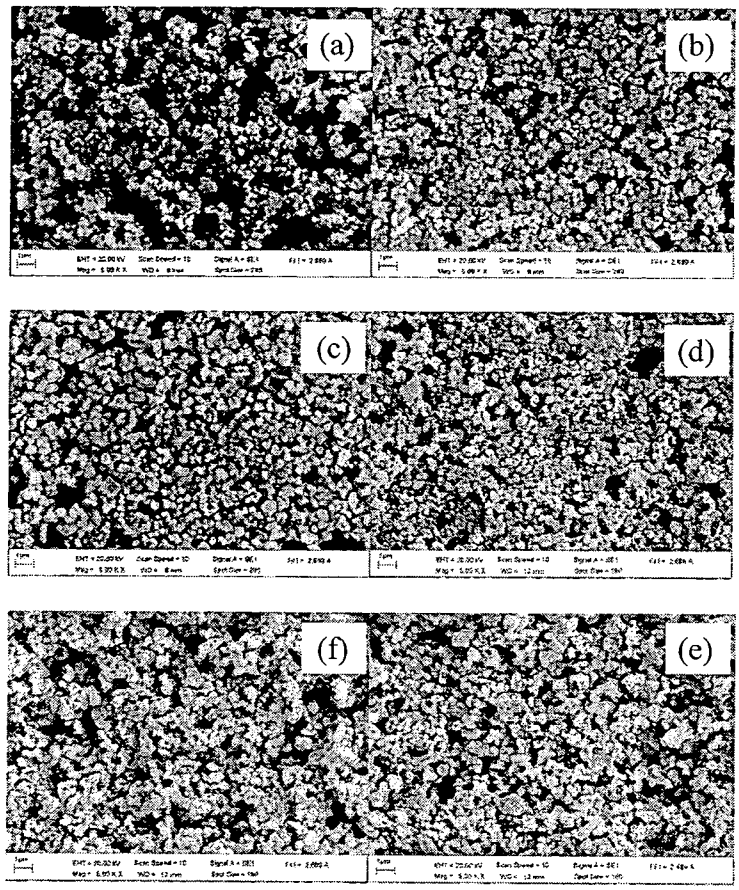

Figure 31 SEM images of BNKFT-0.12/0.03 calcined at (a) 600 °C, (b) 700 °C, (c) 800 °C and BNKFT-0.18/0.01 calcined at (d) 600 °C, (e) 700 °C, (f) 800 °C

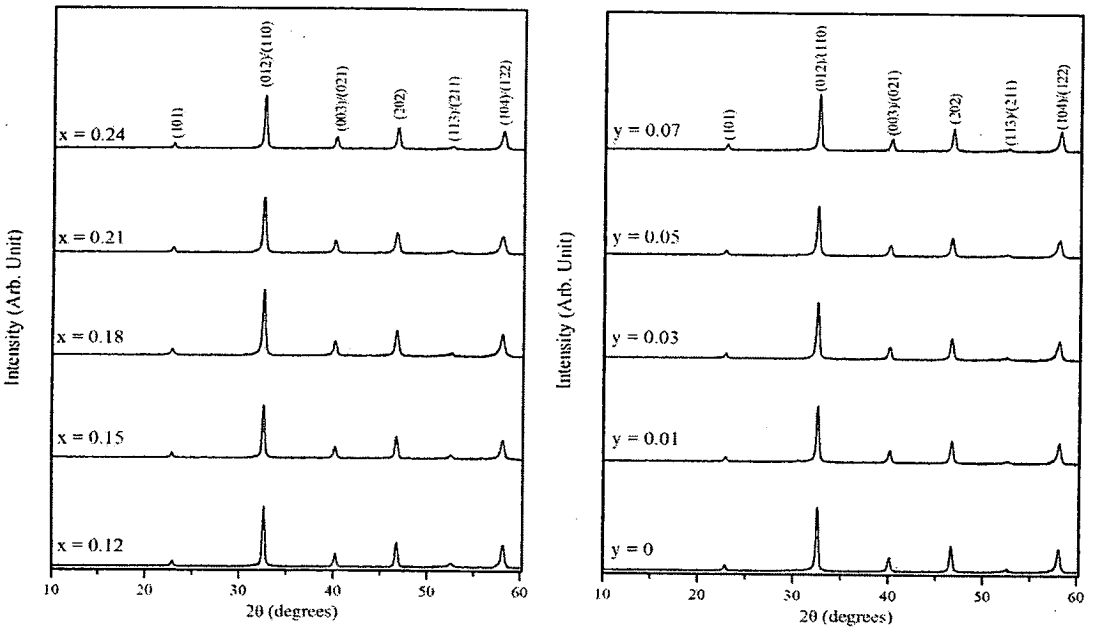

(a) (b)

Figure 32 X-ray diffraction patterns of (a) BNKFT-x/0.03 and (b) BNKFT-0.18/y calcined powders

The SEM micrographs of BNKFT-x/0.03 and BNKFT-0.18/y powders are exhibited in Figure 33(a–c) and 33(d–f), respectively. All the particles are spherical in shape and agglomerated. With an increase of x content from 0.12 to 0.24, the average particle size decreases from 390 nm to 277 nm (Table 6). As the y content increased, the average particle size increased from 285 nm to 310 nm (Table 7).

The TEM micrographs of BNKFT-x/0.03 and BNKFT-0.18/y powders are shown in Fig. 34(a–c) and 34(d–f), respectively. It can be seen that the powder particles have a similar spherical shape and a porous agglomerated form. With an increase of the x content from 0.12 to 0.24, the average particle size decreased from 197 nm to 92 nm. The average particle size increased from 189 nm to 244 nm with an increase of the y content. However, the TEM results were different in their values when compared with the particle size from the SEM image. This may have been caused by the agglomeration affects in the SEM results.

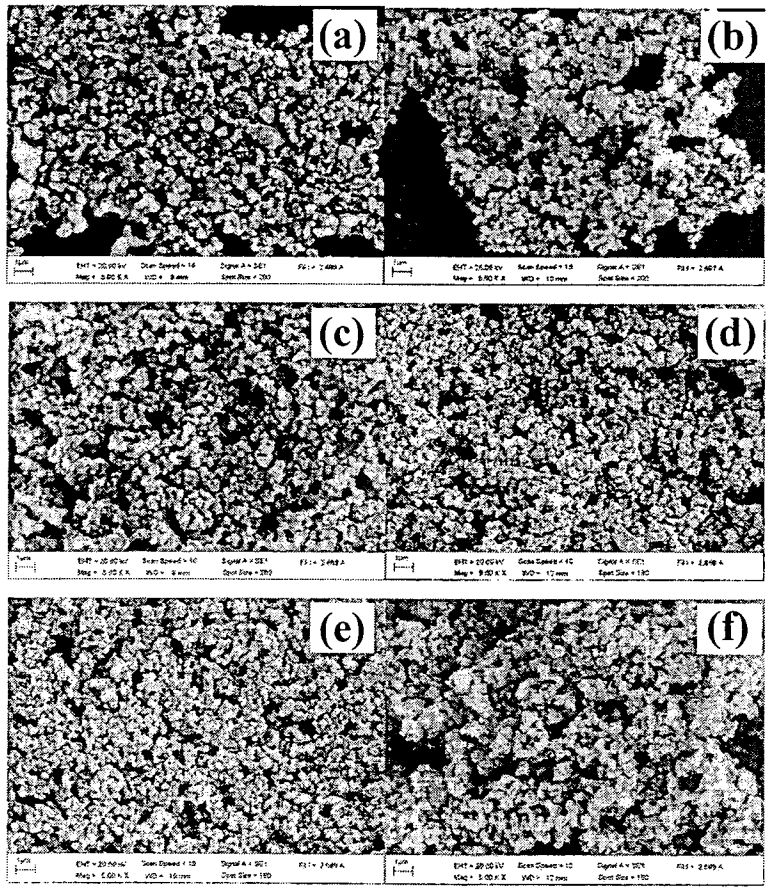

Figure 33 SEM images of BNKFT-x/0.03 calcined powder with (a) x=0.12, (b) x=0.18, (c) x=0.24 and BNKFT-0.18/y calcined powder with (d) y=0, (e) y=0.03, (f) y=0.07

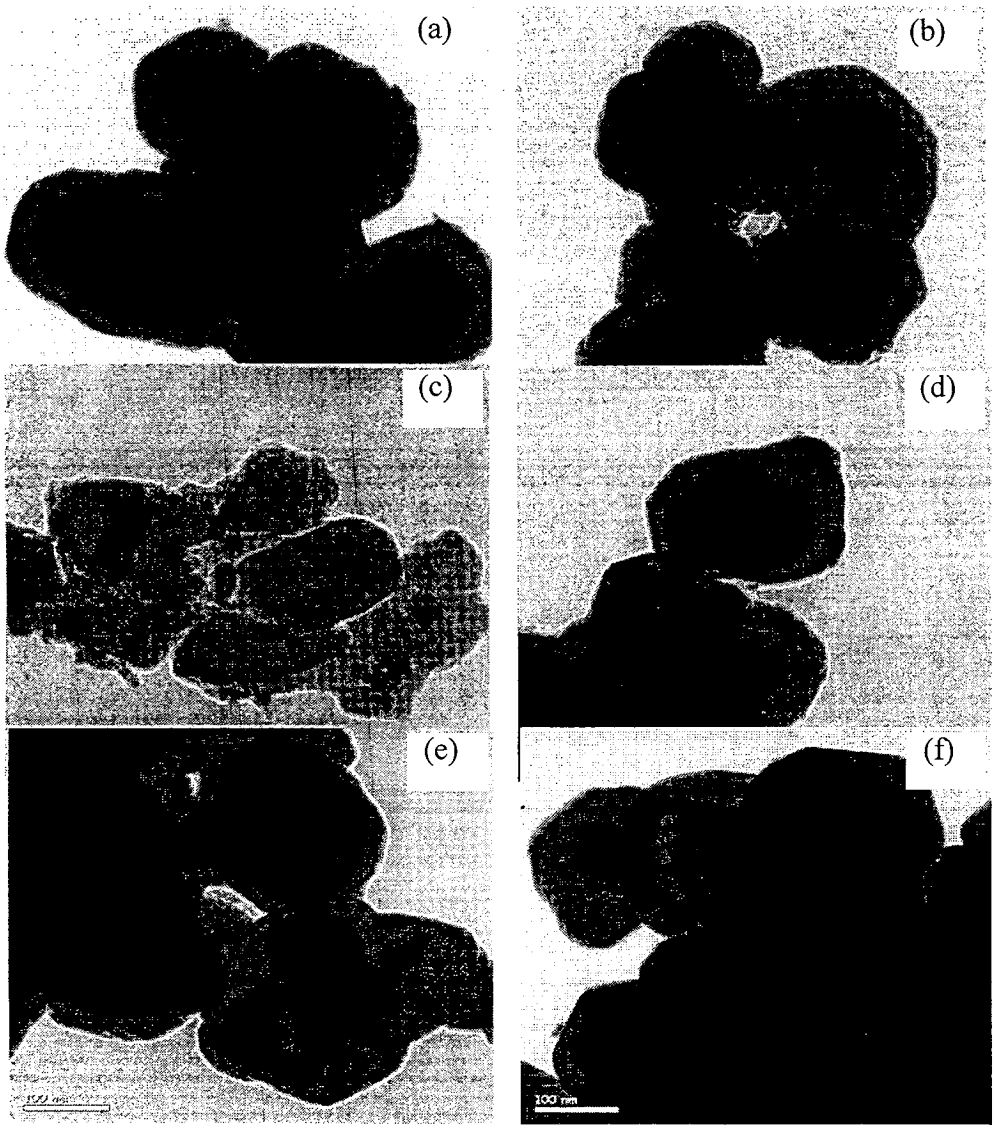

Figure 34 TEM images of BNKFT-x/0.03 calcined powder with (a) x=0.12, (b) x=0.18, (c) x=0.24 and BNKFT-0.18/y calcined powder with (d) y=0, (e) y=0.03, (f) y=0.07

Table 6 Perovskite phase, lattice parameter and average particle size of BNKFT-x/0.03 powders calcined at various temperatures

Composition of x	Calcination temperature (°C)	Perovskite phase (%)	Lattice parameter a (Å)	Average particle size (nm)
0.12	600	87.3	3.8332±0.034	264±15.1
	650	92.7	3.8371±0.032	277±18.4
	700	97.2	3.8376±0.064	297±19.0
	750	100	3.8415±0.063	390±15.2
	800	100	3.8442±0.043	411±16.5
0.15	600	96.5	3.8591±0.041	259±18.1
	650	95.0	3.8597±0.056	266±19.3
	700	95.9	3.8598±0.044	317±17.2
	750	100	3.8602±0.052	296±14.4
	800	100	3.8618±0.034	324±18.3
0.18	600	85.6	3.8562±0.055	236±17.4
	650	96.4	3.8579±0.034	269±17.1
	700	96.9	3.8590±0.034	271±10.5
	750	100	3.8617±0.066	300±19.5
	800	100	3.8628±0.062	309±17.1
0.21	600	95.0	3.8559±0.032	221±11.4
	650	97.4	3.8560±0.036	230±10.2
	700	98.0	3.8581±0.055	255±19.5
	750	100	3.8658±0.037	290±10.4
	800	100	3.8659±0.038	397±17.5
0.24	600	97.6	3.8545±0.065	210±17.5
	650	98.8	3.8575±0.044	233±19.3
	700	99.5	3.8624±0.066	260±18.4
	750	100	3.8696±0.035	277±18.5
	800	100	3.8698±0.062	283±10.1

Table 7 Perovskite phase, lattice parameter and average particle size of BNKFT-0.18/y powders calcined at various temperatures

Composition of y	Calcination temperature (°C)	Perovskite phase (%)	Lacttice parameter a (Å)	Average particle size (nm)
0	600	83.5	3.8112±0.035	231±18.2
	650	93.2	3.8276±0.033	231±19.4
	700	96.2	3.8262±0.045	255±18.5
	750	100	3.8378±0.066	285±19.7
	800	100	3.8402±0.045	293±18.1
0.01	600	80.8	3.8208±0.067	228±17.3
	650	92.7	3.8486±0.023	260±17.4
	700	97.2	3.8562±0.033	291±11.3
	750	100	3.8611±0.055	296±19.4
	800	100	3.8694±0.057	328±19.5
0.03	600	85.6	3.8562±0.033	236±17.5
	650	96.4	3.8579±0.056	269±17.5
	700	96.9	3.8590±0.033	271±10.6
	750	100	3.8617±0.045	300±19.2
	800	100	3.8628±0.066	309±17.0
0.05	600	86.1	3.8697±0.067	216±19.1
	650	91.8	3.8712±0.034	235±11.8
	700	96.2	3.8864±0.045	262±10.1
	750	100	3.8802±0.066	308±19.2
	800	100	3.8802±0.056	309±12.2
0.07	600	80	3.8914±0.067	236±18.6
	650	89.9	3.8864±0.045	251±18.5
	700	96.5	3.9008±0.066	273±10.1
	750	100	3.9013±0.023	310±19.6
	800	100	3.9216±0.033	315±15.3

Effect of sintering temperature and amount of x and yon crystal structure and microstructure of BNKFT ceramics

The XRD diffraction pattern of BNKFT-0.18/0.03 sintered ceramics at various temperatures are shown in Figure35. The X-ray analysis indicated that BNKFT-0.18/0.03 sintered 900 °C to 1075 °C. It can be seen that the BNKFT-0.18/0.03 ceramics possess a single-phase perovskite structure in all samples. All the peaks of the solid solution system were indexed by pattern matching based on JCPDS data on BNT (36-0340) and $Bi_{0.5}K_{0.5}TiO_3$ (36-0339). Generally, the tetragonal structure is characterized by a single peak of (111) between 39 ° and 41° and (002)/(200) peaks splitting between 45° and 48°. Nevertheless, the rhombohedral structure is characterized by (003)/(021) peaks splitting between 39° and 41° and a single peak of (202) between 45° and 48°. At a sintering temperature of 900 °C, the (003)/(021) peaks splitting appears in the 2θ range of 39-41°(Fig. 35(b)) and the (202) peak is asymmetric in the range of 45-48°(Fig. 35(c)). When sintering temperature is increased, the (003)/(021) peak begins to merge into a single (111) peak and the (202) peak starts to split into two peaks of (002)/(200). These results revealed that the crystalline structure has two phases between rhombohedral and tetragonal coexisting and also indicated that the sintering temperature affects the increase of the tetragonal and the decrease of the rhombohedral phases.

The SEM photographs of BNKFT-0.18/0.03 sintered ceramics at various temperatures are shown in Figure36. It was found that increasing sintering temperature helped the growth of grain size. The average grain size increased from 0.37 to 2.49 μm as listed in Table 8. A porous microstructure with small grain size was observed at 950 °C. The increase of sintering temperature significantly encouraged the grain growth and microstructure densification. However, the grain size of the sample sintered above 1050 °C also displayed a high degree of porosity. Moreover, the cross-section microstructure of the samples presented predominantly an inter-granular cleavage with sintering temperature below 1000 °C. At above 1000 °C, the samples changed from inter-granular to intra-granular. This indicated that the sintering temperatures strongly affect grain boundaries.

The density and shrinkage of BNKFT ceramics with sintering temperatures between 900 °C and 1075 °C can also be seen in Table 8. The density and shrinkage increased with increasing sintering temperatures from 900 °C to 1050 °C, and reached a maximum value of 5.85 g/cm^3 (96.9% of theoretical density) and 18.0% at 1050 °C and decreased after further sintering at a higher temperature (1075 °C). The decrease in density of the BNKFT ceramics sintered at a higher temperature (1075 °C) may be due to the potassium and bismuth loss [53, 92], and the presence of a porous microstructure.

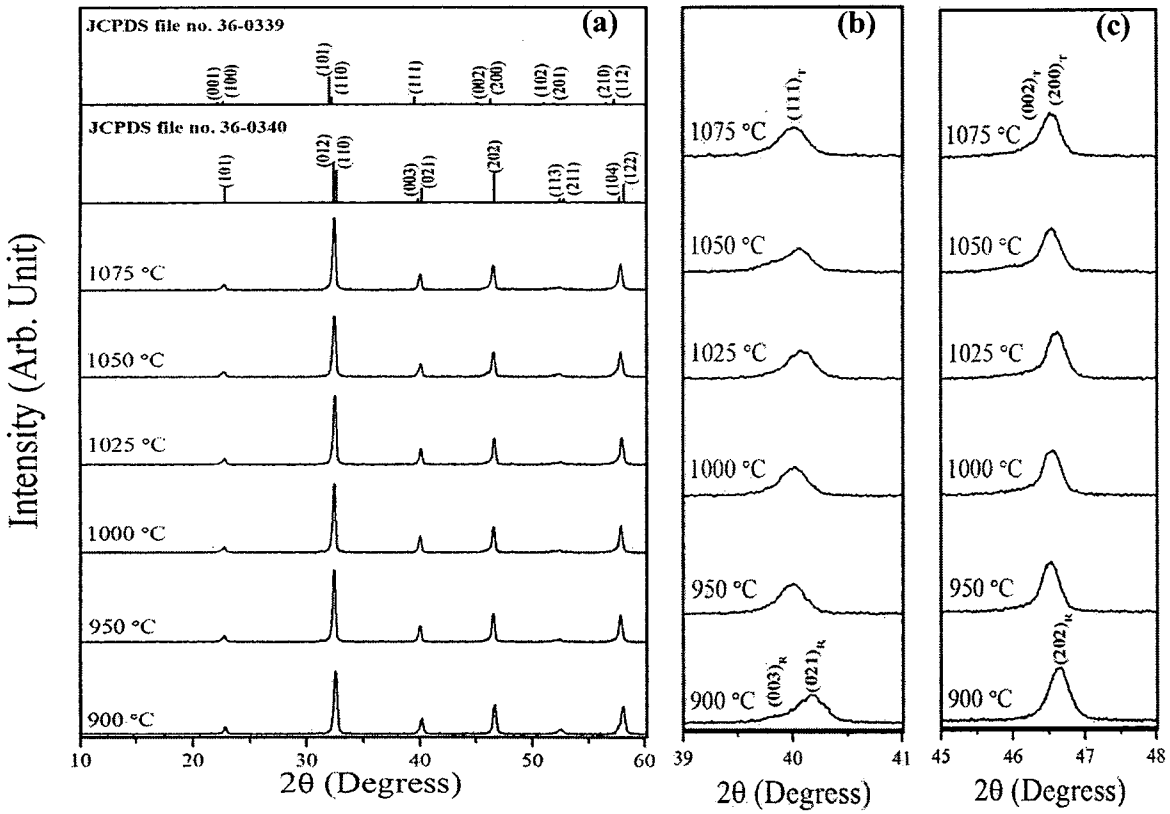

Figure 35 X-ray diffraction patterns of BNKFT0.18/0.03 sintered ceramics at various temperatures in the 2θ range of (a) 10°-60°, (b) 39°-41° and (c) 45°-48°

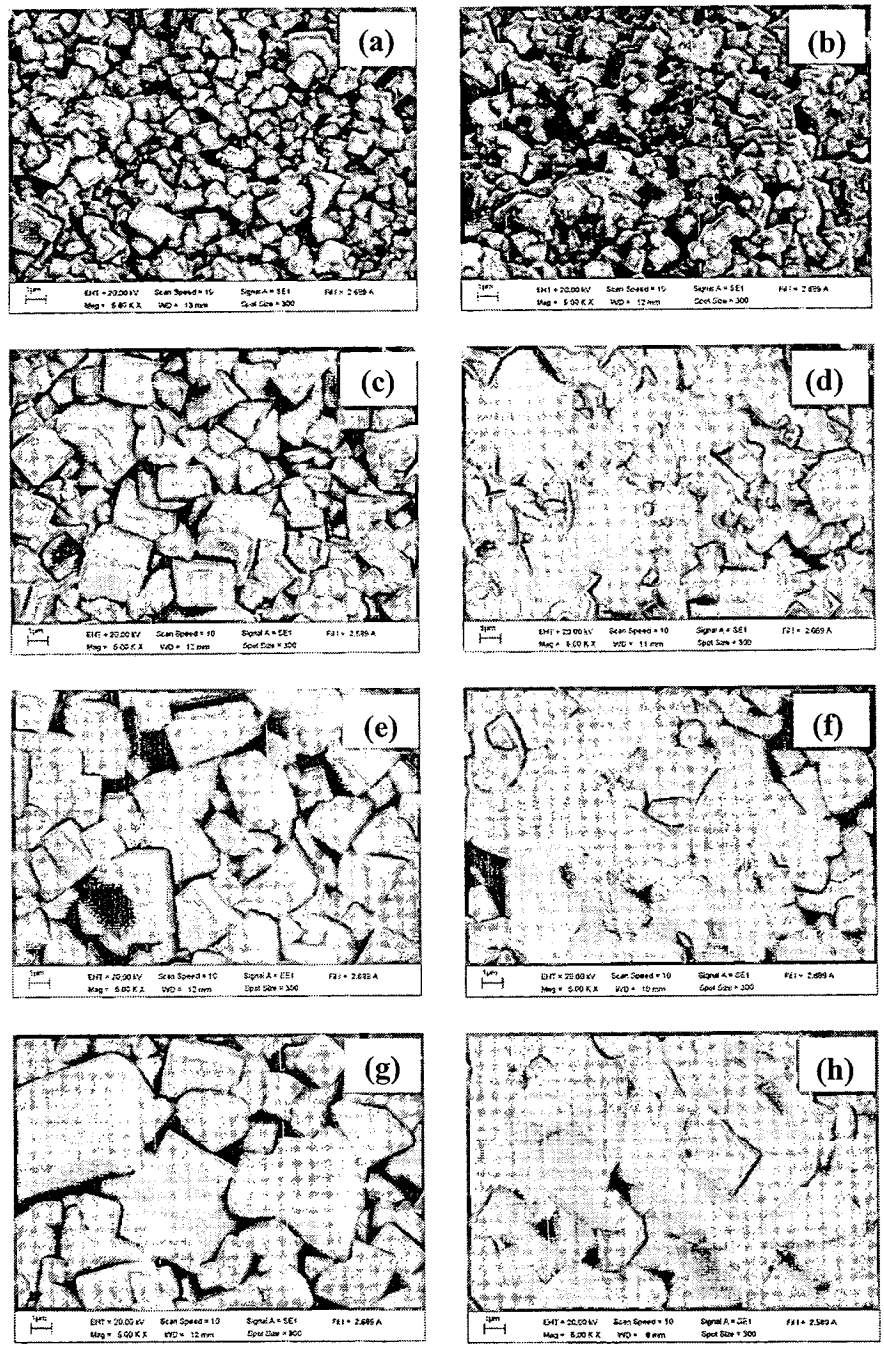

Figure 36 Surface morphologies and cross-sectional micrographs of the BNKFT0.18/0.03 sintered ceramics at various temperatures: (a) and (b) sintered at 950 °C, (c) and (d) sintered at 1000 °C, (e) and (f) sintered at 1050 °C, (g) and (h) sintered at 1075 °C

Table 8 Average grain size, density and shrinkage of BNKFT ceramics at various temperatures

Sintering temperature (°C)	Average grain size (μm)	Measured density (g/cm^{-3})	Relative density (%)	Shrinkage (%)
900	0.37	4.96	82.0	10.9
950	0.49	5.22	86.3	12.3
1000	1.21	5.47	90.4	16.9
1025	1.41	5.77	95.4	17.4
1050	1.59	5.85	96.9	18.0
1075	2.49	5.80	95.8	17.9

The optimum sintering temperature of all samples was found at 1050°C for 2 h, and it was then that the amounts of x and y on the crystal structure and microstructure were examined. The XRD patterns of BNKFT-x/0.03 ceramics are shown in Figure 37(a)-(c). All the samples exhibit a pure perovsktite structure, indicating that K^+ was diffused into the lattice to form a solid solution. In general, the rhombohedral structure is characterized by (003)/(021) peaks spitting between 39° and 41° and a single peak of (202) between 45° to 48° whereas a pure tetragonal structure is characterized by a single peak of (111) between 39° and 41° and (002)/(200) peaks splitting between 45° to 48°. For x=0.12, the (003)/(021) peaks splitting occurs in the 2θ range of 39° to 40°(Figure 37(b)) and the (202) peak is asymmetric in the range of 45° to 47° (Figure 37(c)). When there was an increase of x content, the (003)/(021) peak begin to merge into a single (111) peak and the (202) peak started to split into two peaks of (002)/(200), which revealed that the crystalline structure has two phases between rhombohedral and tetragonal coexisting. Furthermore, the increasing of x content is affected by the increasing of the tetragonal and decreasing of the rhombohedral phase

The XRD patterns of BNKFT-0.18/y ceramics are shown in Figure 38(a)-(c). The entire samples show the pure perovskite structure. For y=0, in the 2θ range of 39° to 41°, the (003)/(021) peaks splitting is slight (Figure 38(b)). The peak splitting

diminishes and begins to merge into a single (111) peak with increasing y content from0 to 0.07. Moreover, in the 2θ range of 45° to 48° of y=0, the peak showed an asymmetric shape (Figure 38(c)). When there was an increase of y content, the peak became more asymmetric and skewed to the left side. These results indicated that the ceramics reveal coexistence between tetragonal and rhombohedral phases. The structure results are in good agreement with previous work [19].

The SEM micrographs of BNKFT-x/0.03 ceramics are shown in Figure 39 (a-c). All ceramics show a quasi-cubic morphology with clear grain boundaries. The average grain size decreases from 2.67 μm to 0.98 μm when the x content was increased from 0.12 to 0.24, as listed in Table 9. The grains become evidently smaller with increasing x content, which can be explained by the K^+ ion concentrates near grain boundaries and substantially reduced mobility as densification occurred. The decrease in the mobility of the grain boundary weakens the mass transport. As a result, grain growth is obviously inhibited and smaller grains are formed in the ceramic samples at a high concentration of x[17].

The SEM photomicrographs of BNKFT-0.18/y sintered pellets are shown in Figure 39(d)-(f). It can be seen that the grain exhibits an almost quasi-cubic morphology. The average grain size increased from 2.15 μm to 2.81 μm when increasing of y content (Table 9). The increased in grain size of the ceramics are due to the Fe^{3+} entering into the sixfold coordinated B-site to substitute for Ti^{4+} because of radius matching [19]. The densities of BNKFT-0.18/y ceramics with different y content are listed in Table 9.

The measured density and relative density of the BNKFT-x/0.03 ceramics with different x content are listed in Table 9. The density increased and reached a maximum value of 5.85 g/cm^{-3} or ~ 96.6 % of the theoretical density obtained from the sample with x = 0.18, and slightly decreased with x > 0.18 (Table 9). The densityincreased from 5.57 g/cm^{-3} to 5.85 g/cm^{-3} (93.1% - 96.4% of theoretical density) when concentration of x increased from 0 to 0.03, and then dropped to 5.77 g/cm^{-3} (93.9% of theoretical one) with further increasing of y to 0.07.

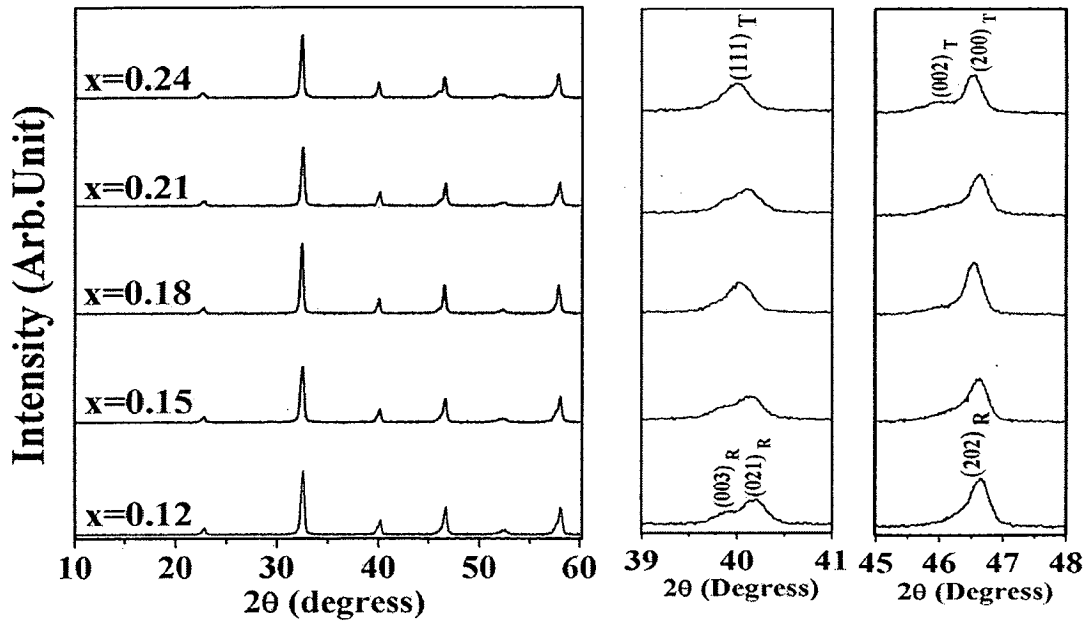

Figure 37 X-ray diffraction patterns of BNKFT-x/0.03 sintered ceramics in the 2θ rang of (a) 10° to 60°, (b) 39° to 41° and (c) 45° to 48°

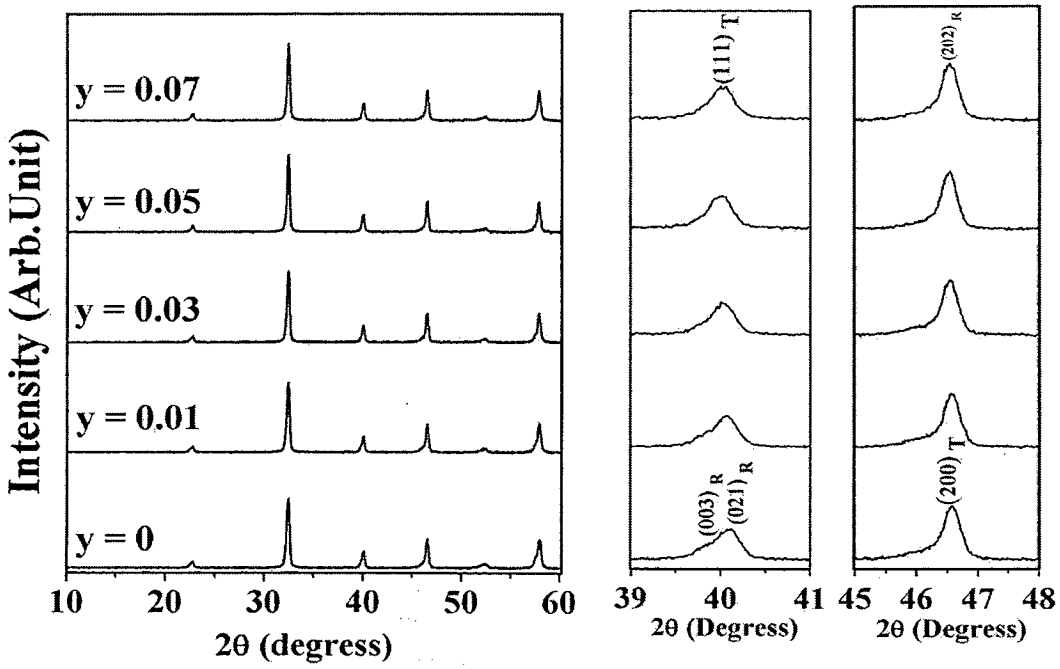

Figure 38 X-ray diffraction patterns of BNKFT-0.18/y sintered ceramics

Effect of x and y on electrical properties of BNKFT Ceramics

I. Dielectric properties of BNKFT ceramics

Figure 40(a) shows the temperature dependence of the dielectric constant (ε_r) of BNKFT-x/0.03 ceramics which were measured at 1 kHz. The dielectric constant showed two peaks (T_d at low temperature and T_c at high temperature) in all samples. The T_d is the temperature at which the phase transition from ferroelectric (rhombohedral) to anti-ferroelectric (tetragonal) occurred. T_c is the temperature at which the transition from tetragonal anti-ferroelectric (tetragonal) to cubic paraelectric (cubic) occurred. When there was an increase of x, T_d of the sample shifted to the lower temperature from 185 °C to 94 °C whereas T_c shifts to higher temperature regions from 282° to 321 °C, as shown in Figure 40(a). At Curie temperature, the maximum dielectric constant was observed in all samples. It tended to increase from 5,890 to 7,850 when the x content increased from 0.12 to 0.18. When further increasing x content to 0.24, ε_r decreased to 3,750, as listed in Table 9. The dielectric loss at T_c tended to decrease from 0.04 to 0.02 when the x content increased from 0.12 to 0.24, as shown in Table 9.

Temperature dependence of the dielectric constant (ε_r) of BNKFT-0.18/y ceramics which were measured at 1 kHz is shown in Figure 40(b). There are two abnormal temperature peaks which existed in all samples with different compositions. The T_d and T_c shifts to lower temperature regions from 131 °C to 123 °C and 294 °C to 282 °C with increasing y content from 0 to 0.07, as shown in Figure 40(b). The result agrees with the result of Zhou et al[18]. At T_c, the maximum dielectric constant tended to increase in value from 5,630 to 7,850 when the y content increased from 0 to 0.03. After that, the maximum dielectric constant of ceramics decreased as the concentration of y increased above 0.03, as listed in Table 9. The dielectric loss at T_c tended to increase from 0.02 to 0.04 when the y content increased from 0 to 0.07, as shown in Table 9. The ε_r and tanδ at T_c (at 1 kHz) of all compositions is closely consistent with the result of previous work [8].

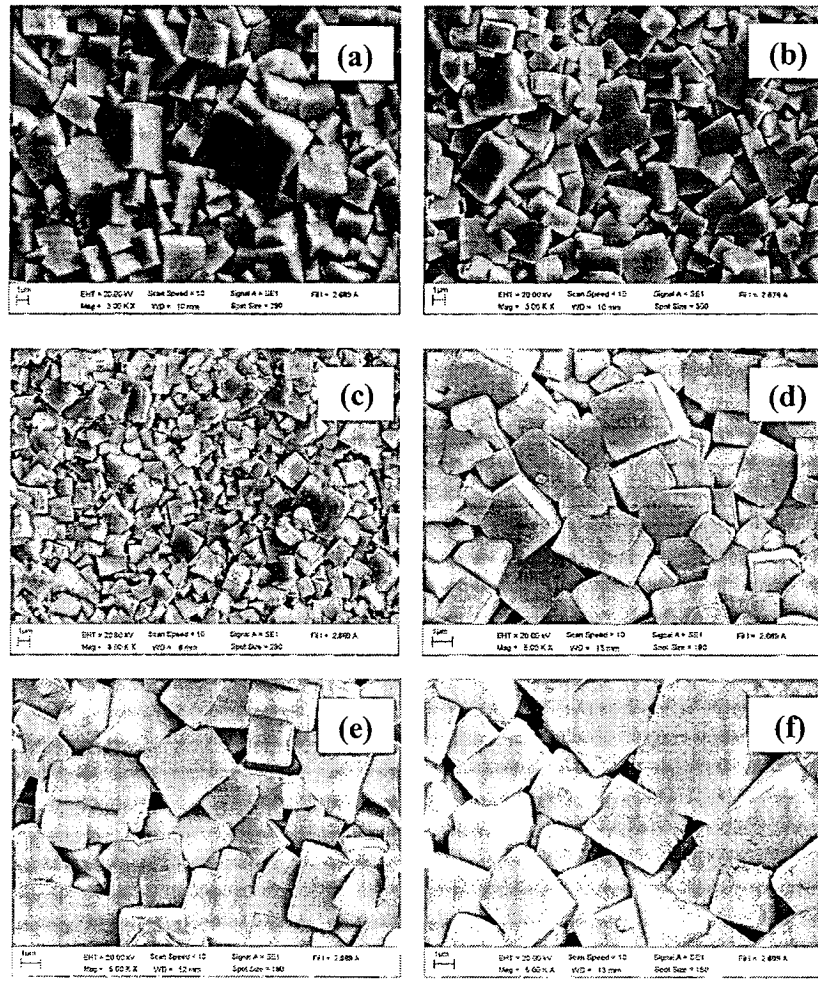

Figure 39 SEM images of BNKFT-x/y sintered ceramics with (a) x= 0.12, (b) x=0.18, (c) x=0.21, (d) y=0, (e) y=0.03 and (f) y=0.07

II. Ferroelectric properties of BNKFT ceramics

The ferroelectric polarization–electric field (P-E) loop of BNKFT-x/0.03 ceramics measured at 40 kV/cm is shown in Figure 41(a). All of composition, the P-E loops were not fully saturated. In literature of BKT (x) composition observation of saturated P-E behavior is reported to be difficult [64-66]. The measured remnant polarization (P_r) of BNKFT-x/0.03 ceramics increased from 14.7μC/cm^2 to the maximum value (18.6μC/cm^2) at x=0.18, and then dropped to 4.4μC/cm^2 with a further increase of x to 0.24. It is clear from P-E data that small additions of K^+ (up to x=0.18) improves the remnant polarization (P_r) values. The partial substitution

of Na^+(1.39 Å)ions by K^+ (1.64 Å) ions that have difference in ionic radii could cause distortion of unit cell, leading to the structure distortion of the oxygen octahedral and thus resulting in an increase of P_r. However, the decrease in P_r as x content increased (x>0.18) suggests that the high substitutions of K^+ ions for Na^+ ions would cause the decrease in relative displacement of unit cells. The ferroelectric polarization–electric field (P-E) loop of BNKFT-0.18/y ceramics is shown in Figure 41(b). Typical rectangular loop can be observed for the BNKFT-0.18/0. With the y increased to 0.07, obviously pinched P-E loop can be observed. At y=0, P_r and E_c is ~24.6 μC/cm^2 and ~22.4 kV/cm, respectively. With a further increase in y content to 0.07, $P_r$decrease to 7.6 μC/cm^2, as listed in Table 9.

III. Piezoelectric properties of BNKFT ceramics

The piezoelectric coefficients of BNKFT-x/0.03 ceramics are illustrated in Figure 42(a). The piezoelectric coefficients d_{33} of all ceramics first increased and then decreased with increasing x content. The maximum d_{33} are obtained at x=0.18, which is 213 pC/N. The decrease of d_{33} due to the clamping effect association with oxygen vacancies hinders sufficient reorientation of ferroelectric domains during electrical poling. The d_{33} at x=0.18 showed a value higher than the result of previous work [19]. The piezoelectric coefficient of BNKFT-0.18/y ceramics is shown in Figure 42(b). When y=0, the piezoelectric coefficients d_{33} are 164 pC/N. With increasing content of y, d_{33} reached the maximum values of 213 pC/N at y=0.03, and then dropped in value.

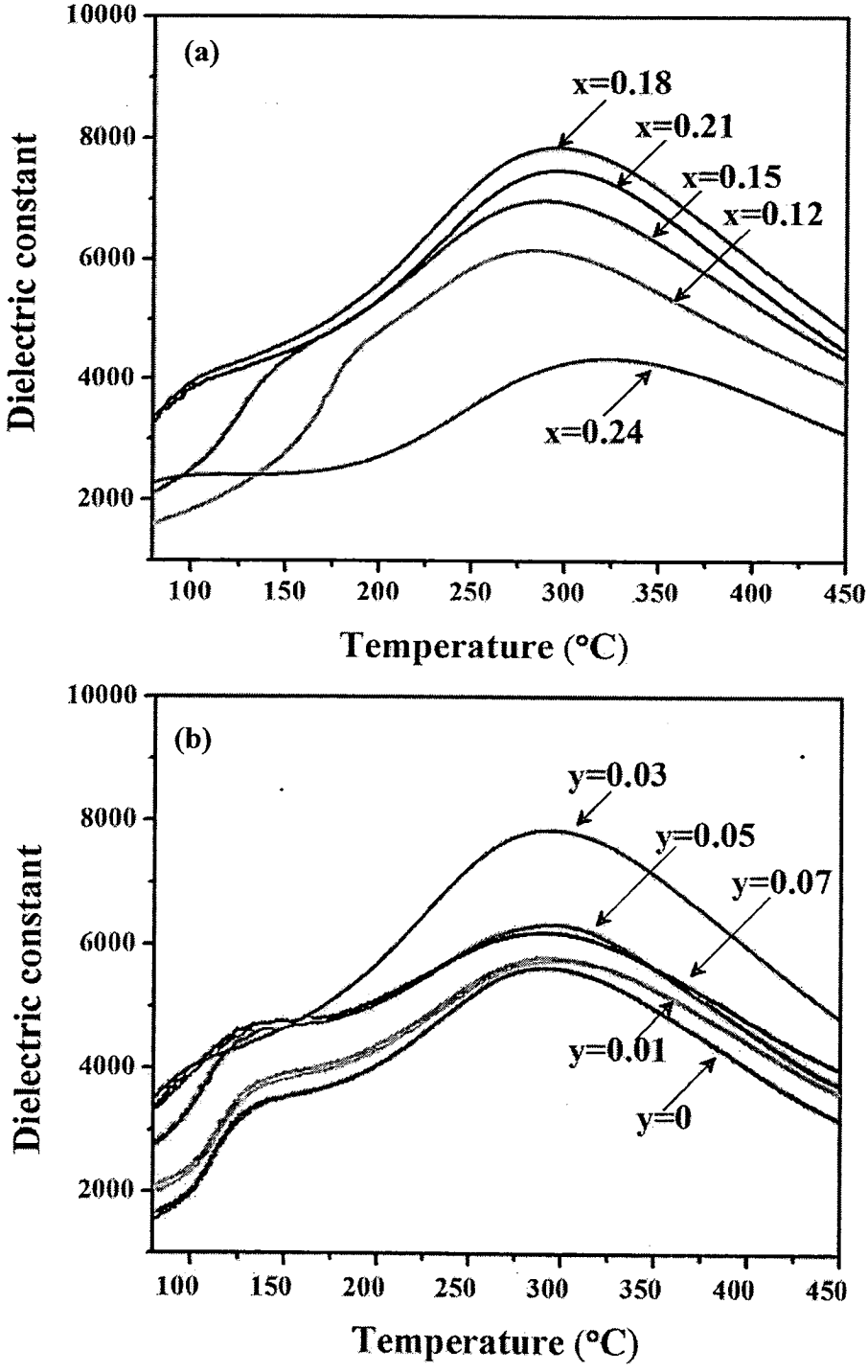

Figure 40 The temperature dependences of dielectric constant (ε_r) of the (a) BNKFT-x/0.03 and (b) BNKFT-0.18/y ceramics

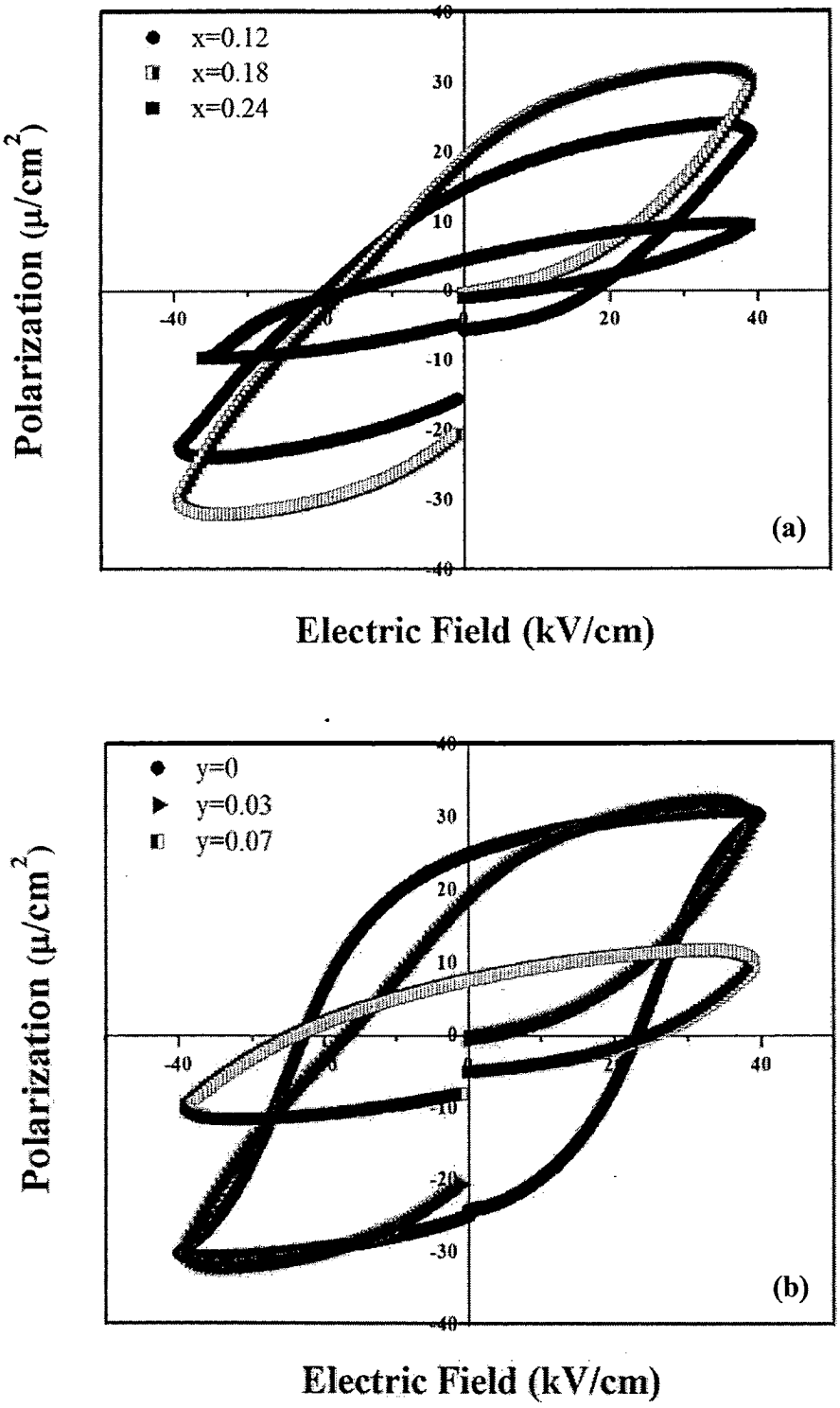

Figure 41 Ferroelectric hysteresis loops of (a) BNKFT-x/0.03 and (b) BNKFT-0.18/y ceramics

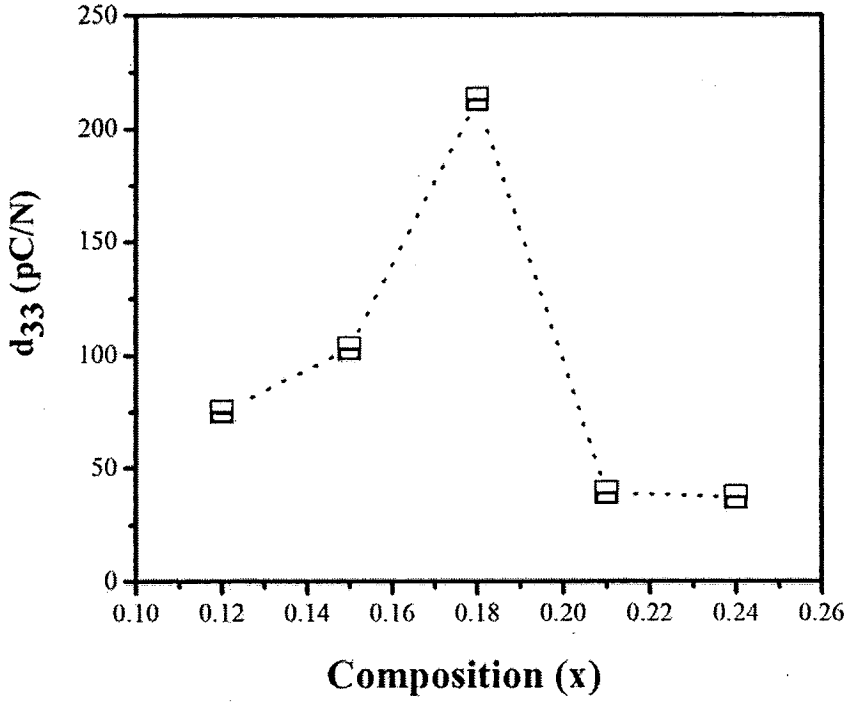

(a)

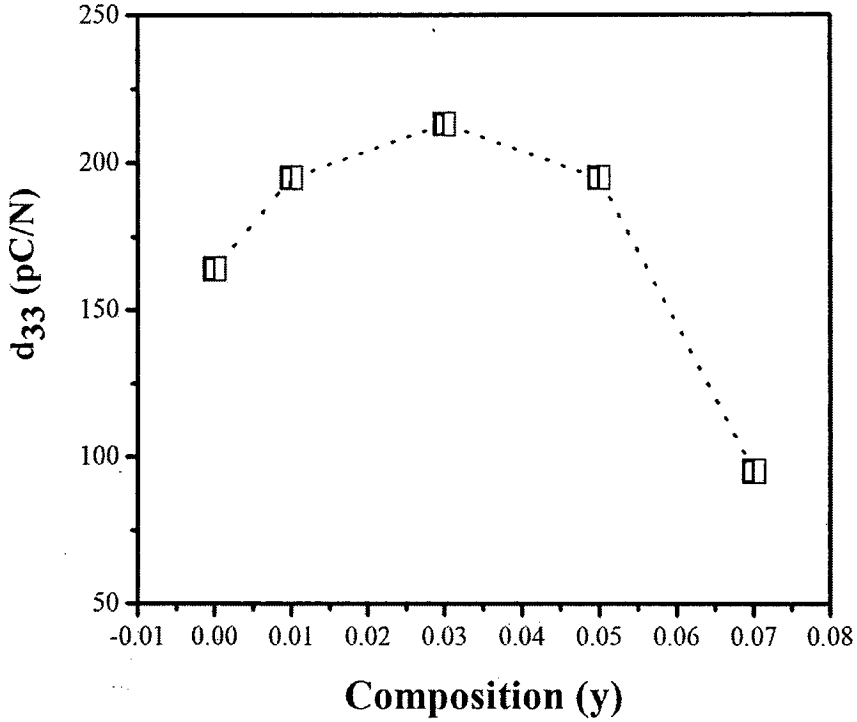

(b)

Figure 42 Piezoelectric properties of (a) BNKFT-x/0.03 and (b) BNKFT-0.18/y ceramics

Table 9 Average grain size, density, dielectric constant (ε_r), dielectric loss (tanδ), remnant polarizations (P_r) and coercive fields (E_c) of BNKFT-x/y ceramics

Composition	Average grain size (μm)	Measured density (g/cm^3)	Relative density (%)	ε_r at T_c	tanδ at T_c	P_r ($\mu C/cm^2$)	E_c (kV/cm)
x=0.12	2.67	5.73	94.6	5,890	0.04	14.7	19.0
x=0.15	2.41	5.79	95.7	6,970	0.03	18.0	23.8
x=0.18	2.39	5.85	96.6	7,850	0.02	18.6	16.3
x=0.21	1.33	5.79	94.1	7,310	0.02	24.2	24.2
x=0.24	0.98	5.57	92.1	3,750	0.02	4.4	15.2
y=0	2.15	5.57	93.1	5,630	0.02	24.6	22.4
y=0.01	2.23	5.63	93.8	5,640	0.02	19.6	21.9
y=0.03	2.44	5.85	96.4	7,850	0.02	18.6	16.9
y=0.05	2.73	5.80	95.1	6,330	0.03	17.2	24.4
y=0.07	2.81	5.77	93.9	6,320	0.04	7.6	24.7

Conclusions

Lead free BNKFT ceramics were synthesized by the combustion technique. The optimal calcination andsintering conditions were found to be 750 °C for 2 h and 1050 °C for 2 h,respectively. The calcination and sintering temperatures directly affected the phase formation, microstructure, density and electrical properties. The highest density (ρ = 5.85 g/cm^3), superior dielectric properties at T_c (ε_r =7,846 and tanδ = 0.02) and piezoelectric constant (d_{33} =213 pC/N) were obtained from the sample sintered at 1050 °C. With superior electric properties, this work indicates that the BNKFT ceramics prepared by the combustion technique are better than the BNKFT produced by solid stated method.

The content of x and y have a strong influence on the crystal structure, microstructure, lattice parameter and percentage of the perovskite phase of the calcined powders. The lattice parameter of a increased with increasing x andy content. The ceramics possessa pure single phase of perovskite structure, indicating that K^+ and Fe^+ have diffused into the lattice.The SEM images indicated that with increasing x content, particle size decreases. But with increasing y content, the variation of the particle size is opposite. BNKFT powders can be successfully synthesized by the combustion technique at a lower calcination temperature than those prepared by the solid-state reaction method.

The variation of x and y content affects directly crystal structure, microstructure, density, dielectric, ferroelectric and piezoelectric properties of the BNKFT-x/0.03 and BNKFT-0.18/y ceramics. The XRD indicated that the ceramics possess pure single phase of perovskite structure, indicating that K^+ and Fe^+ have diffused into the lattice. With increasesx and y contents, grain size decreases and increase, respectively. The optimum electric properties can be obtained at x=0.18 and y =0.03, as follows: ρ = 5.85 g/cm^{-3}, ε_r = 7,850, tanδ = 0.02, P_r=20.1 μC/cm^2 (measured at 40 kV/cm) and d_{33} = 213 pC/N. With superior electric properties, this work indicates that the BNKFT-x/y ceramics prepared by combustion technique are better than the BNKFT-x/y ceramics prepared by solid state.